

Article

# Maltol- and allomaltol-derived oxidopyrylium ylides: Methyl substitution pattern kinetically influences [5 + 3] dimerization versus [5 + 2] cycloaddition reactions

Lauren P. Bejcek, Aswin K. Garimallaprabhakaran, Duygu M. Suyabatmaz, Alexander Greer, William H. Hersh, Edyta M. Greer, and Ryan Patrick Murelli

*J. Org. Chem.*, **Just Accepted Manuscript** • DOI: 10.1021/acs.joc.9b02137 • Publication Date (Web): 11 Oct 2019

Downloaded from pubs.acs.org on October 12, 2019

## Just Accepted

"Just Accepted" manuscripts have been peer-reviewed and accepted for publication. They are posted online prior to technical editing, formatting for publication and author proofing. The American Chemical Society provides "Just Accepted" as a service to the research community to expedite the dissemination of scientific material as soon as possible after acceptance. "Just Accepted" manuscripts appear in full in PDF format accompanied by an HTML abstract. "Just Accepted" manuscripts have been fully peer reviewed, but should not be considered the official version of record. They are citable by the Digital Object Identifier (DOI®). "Just Accepted" is an optional service offered to authors. Therefore, the "Just Accepted" Web site may not include all articles that will be published in the journal. After a manuscript is technically edited and formatted, it will be removed from the "Just Accepted" Web site and published as an ASAP article. Note that technical editing may introduce minor changes to the manuscript text and/or graphics which could affect content, and all legal disclaimers and ethical guidelines that apply to the journal pertain. ACS cannot be held responsible for errors or consequences arising from the use of information contained in these "Just Accepted" manuscripts.

# Maltol- and allomaltol-derived oxidopyrylium ylides: Methyl substitution pattern kinetically influences [5 + 3] dimerization versus [5 + 2] cycloaddition reactions

Lauren P. Bejcek,<sup>a,b</sup> Aswin K. Garimallaprabhakaran,<sup>a</sup> Duygu M. Suyabatmaz,<sup>a</sup> Alexander Greer,<sup>a,b</sup> William H. Hersh,<sup>b,d</sup> Edyta M. Greer,<sup>c,\*</sup> Ryan P. Murelli<sup>a,b,\*</sup>

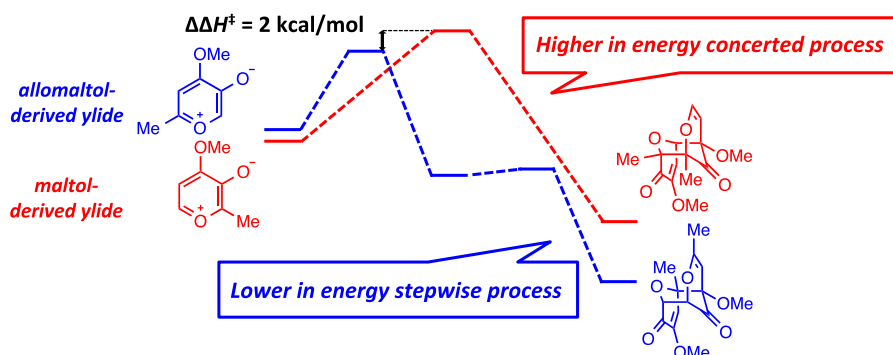
<sup>a</sup> Department of Chemistry, Brooklyn College, The City University of New York, Brooklyn, NY, USA

<sup>b</sup> PhD Program in Chemistry, The Graduate Center of the City University of New York, New York, NY, USA

<sup>c</sup> Department of Natural Sciences, Baruch College, City University of New York, New York, NY, USA

<sup>d</sup> Department of Chemistry and Biochemistry, Queens College, City University of New York, Queens, NY, USA

Contact emails – [edyta.greer@baruch.cuny.edu](mailto:edyta.greer@baruch.cuny.edu) and [rpmurelli@brooklyn.cuny.edu](mailto:rpmurelli@brooklyn.cuny.edu)

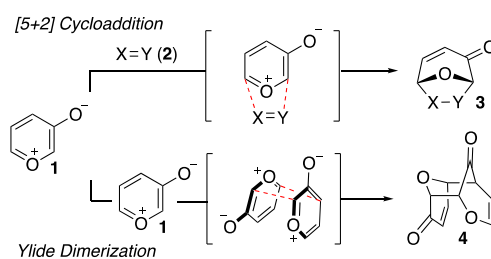


**Abstract.** Oxidopyrylium ylides are useful intermediates in synthetic organic chemistry because of their capability of forming structurally complex cycloadducts. They can also self-dimerize via [5 + 3] cycloaddition, which is an oft-reported side reaction that can negatively impact [5 + 2] cycloadduct yields and efficiency. In select instances, these dimers can be synthesized and used as the source of oxidopyrylium ylide, although the generality of this process remains unclear. Thus, how the substitution pattern governs both dimerization and cycloaddition reactions are of fundamental interest to probe factors to regulate them. The following manuscript details our findings that maltol-derived

oxidopyrylium ylides (*i.e.*, with *ortho* methyl substitution relative to oxide) can be trapped prior to dimerization more efficiently than the regioisomeric allomaltol-derived ylide (*i.e.*, with an *para* methyl substitution relative to oxide). DFT studies provide evidence in support of a steric (kinetically) controlled mechanism, whereby gauche interactions between appendages of the approaching maltol-derived ylides are privileged by higher barriers for dimerization, and thus are readily intercepted by dipolarophiles *via* [5 + 2] cycloadditions.

## Introduction

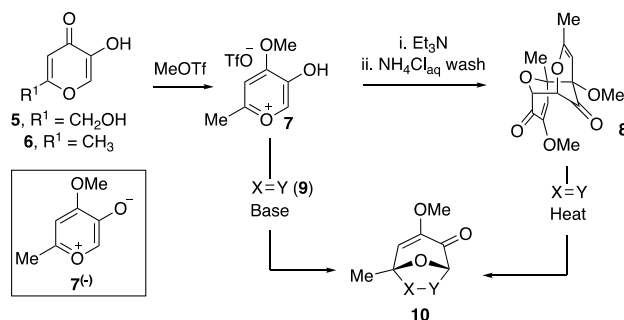
[5 + 2] Cycloaddition reactions between oxidopyrylium ylide intermediates and dipolarophiles generate bicyclic compounds of synthetic use (*i.e.*, **1** → **3**, **Scheme 1**), including highly functionalized natural products.<sup>1</sup> Oxidopyrylium ylide intermediates also have the capacity to dimerize through a [5 + 3] cycloaddition in their neutral form (*i.e.*, **1** → **4**, **Scheme 1**),<sup>2,3</sup> which is an important process that is in need of more study. A mechanistic understanding of factors that influence oxidopyrylium ylide dimerization is potentially of high value due to the difficulty in controlling the otherwise reactive state of the neutral form.



**Scheme 1.** General representation of oxidopyrylium [5 + 2] cycloaddition chemistry, and the known dimerization product of oxidopyrylium ylide **1**.

Our lab has previously focused on intermolecular [5 + 2] cycloaddition reactions with oxidopyrylium ylides generated via deprotonation of kojic acid (**5**)-derived methyl triflate salts (**Scheme 2**), first described by Wender.<sup>3</sup> During the course of these studies, it was revealed that dimer **8** generally forms instantaneously upon treatment of base, even in the presence of reactive dipolarophiles, but over time can convert into cycloadducts (*i.e.*, **10**).<sup>4</sup> While it has been proposed that the conversion of the oxidopyrylium dimer to

cycloaddition products proceeds by way of cycloreversion back to oxidopyrylium ylides (*i.e.*, **7<sup>(-)</sup>**),<sup>5</sup> a confounding problem in the validation of this mechanistic hypothesis has been the inability to directly detect the ylides due to their highly reactive nature. The purification of oxidopyrylium dimer furthermore provides a source of oxidopyrylium ylide free of the Brønsted acid and base, and has been advantageous in reaction optimization<sup>6</sup> and total synthesis efforts.<sup>7</sup> However, it should be noted that high temperatures and/or prolonged reaction times are needed which can present a potential limitation. Thus, understanding how specific structural features influence relative rates of oxidopyrylium ylide dimerization and cycloaddition reactions is of fundamental importance.



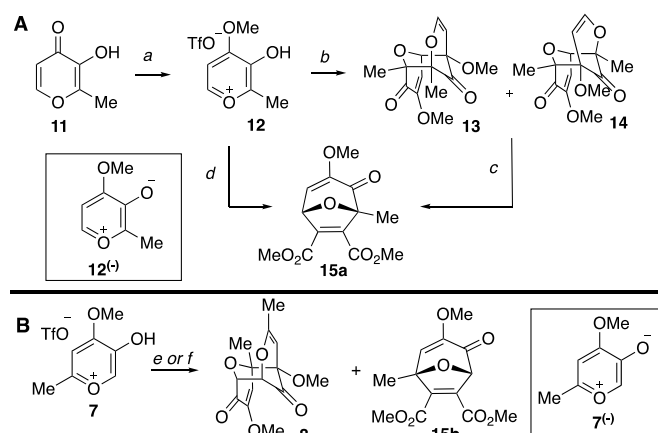
**Scheme 2. Kojic acid-derived oxidopyrylium salt **7** and strategies for its usage in oxidopyrylium cycloaddition chemistry**

Herein we present experimental and theoretical results on factors that control the dimerization versus cycloaddition behavior of regioisomeric maltol and allomaltol-derived oxidopyrylium ylides. Specifically, we demonstrate that (i) maltol-derived oxidopyrylium ylide (see **12<sup>(-)</sup>** in **Scheme 3** for details) is more rapidly trapped by dipolarophiles, such as dimethyl acetylenedicarboxylate (DMAD, **16a**), than the allomaltol-derived ylide (**7<sup>(-)</sup>**); (ii) DFT calculations show that homo-dimerization of maltol-derived oxidopyrylium ylide (**12<sup>(-)</sup>**  $\rightarrow$  **13/14**, **Scheme 3**) proceeds through a concerted process, whereas homo-dimerization of allomaltol-derived oxidopyrylium ylide (**7<sup>(-)</sup>**  $\rightarrow$  **8**) proceeds through a two-step process that is lower in energy; (iii) Kinetic studies for the reaction between homodimers (**8/13/14**) and DMAD (**16a**) to form [5 + 2] cycloaddition products reveal different kinetic profiles for the reaction with **8**, and that

with **13/14**, but are each consistent with a mechanism involving full cycloreversion to the oxidopyrylium ylide; and (iv) Studies with dipolarophiles are presented to gauge the [5 + 2] cycloaddition trapping efficiencies of the ylides prior to [5 + 3] dimerization.

## Results and Discussion.

*Initial Observations Illustrating Dramatic Reactivity Differences Between Maltol and Allomaltol-Derived Oxidopyrylium Ylides.* Our studies began with an evaluation of maltol-derived oxidopyrylium ylides (**12**<sup>+</sup>, **Scheme 3A**), which were absent from the literature with the exception of a single report by Li.<sup>8</sup> Upon synthesizing the maltol-derived oxidopyrylium salt (**12**) and treating it to triethylamine, we found that two dimers formed in approximately 2:1 ratio (**12** → **13** + **14**, **Scheme 3A**). This result differed from the analogous dimerization of allomaltol-derived salt **7**, which led exclusively to a single isomer, **8** (**Scheme 3B**). Both dimers **13** and **14** reacted with DMAD (**16a**) at higher temperatures, affording oxidopyrylium cycloaddition product **15a**, confirming that these regioisomeric dimers could be used as an ylide source. However, the reactions were noticeably more sluggish than was expected based on our experience with the analogous reaction with dimer **8**. In fact, the reaction between either dimer **13** or **14** with DMAD (**16a**) only reached ~70% conversion after 8 h at 100 °C as compared to full conversion within 5 min with dimer **8** in closely related studies (**Scheme 3B**).<sup>4</sup> Consistent with these findings, a competition experiments in which a 1:1 mixture of **8** and **13/14** heated in the presence of **16a** and monitored over time led first to formation **15b**, followed by formation of **15a**. Therefore in order to promote a higher yielding process for the cycloaddition with **13/14** and **16a**, the reaction was carried out at elevated temperatures (150 °C), which provided **15a** in 95% yield after only 2 h (**Scheme 3A**).



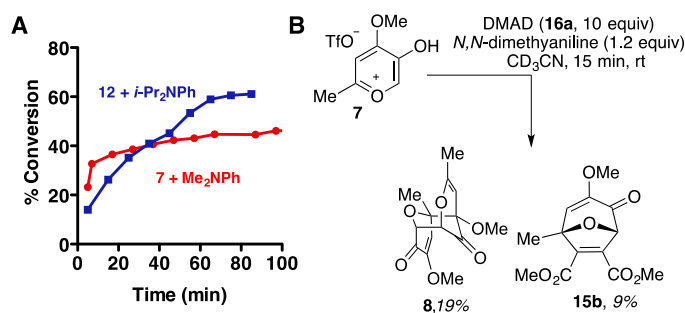
- a. Methyl trifluoromethanesulfonate (1.5 equiv.),  $\text{CH}_2\text{Cl}_2$ , reflux, 4 hours, 54%.  
 b. Triethylamine (1.2 equiv.),  $\text{CH}_2\text{Cl}_2$ , rt, 2 hours, (45% **13**, 25% **14**).  
 c. Dimethylacetylene dicarboxylate (DMAD, **16a**, 11 equiv.),  $\text{CDCl}_3$ ,  $\mu\text{wave}$ , 150 °C, 2 hr, 95% **15a**.  
 d. DMAD (**16a**, 5 equiv.),  $\text{CD}_3\text{CN}$ , then *N,N*-diisopropylaniline (1.2 equiv.), rt, 30 min, 94% **15a**, 5% **13/14**. Yields based on  $^1\text{H}$  NMR.  
 e. DMAD (**16a**, 5 equiv.),  $\text{CD}_3\text{CN}$ , then *N,N*-diisopropylaniline (1.2 equiv.), rt, 5 min, 82% **8**, 4% **15b**. Yields based on  $^1\text{H}$  NMR..  
 f. *N,N*-diisopropylaniline (1.2 equiv.), DMAD (**16a**, 20 equiv.),  $\mu\text{wave}$ , 100 °C, 5 min, 90% **15b**. (see ref. 4 for details)

**Scheme 3. Observed differences of [5 + 2] cycloadditions of (A) maltol and (B) allomaltol-derived oxidopyrylium salts with dimethyl acetylenedicarboxylate (16a)**

The more sluggish reactivity between dimer **13** and **14** with DMAD (**16a**) were surprising to us, especially in light of findings by Li that a closely analogous reaction between **12** and the presumably less reactive indole was completed within 7 h at room temperature.<sup>8</sup> Upon closer examination, when a  $\text{CD}_3\text{CN}$  solution containing a mixture of oxidopyrylium salt **12** and DMAD (**16a**) was subsequently treated with *N,N*-diisopropylaniline, after only 30 minutes at room temperature, **15a** was the major product, and dimers **13** and **14** were only observed as minor products (**12** → **15a**, **Scheme 3A**), more closely consistent with the Li studies. The result, however, was highly contradictory to our experience with regioisomeric salt **7**, where dimer **8** is almost always observed as the major product upon addition of base in the presence of dipolarophiles, and over time or at elevated temperature converts to cycloaddition products (**7** → **8** → **15b**, **Scheme 3B**). Likewise, competition experiments in which a 1:1 mixture of **7** and **12** in the presence of **16a** are treated to *N,N*-diisopropylaniline and monitored over time via

$^1\text{H}$  NMR, resulted in only the appearance of dimer **8** (from **7**) and DMAD cycloadduct **15a** (from **12**).

Given these findings, the dimerization processes were evaluated in the absence of DMAD (**16a**). Consistent with prior experiences,<sup>4</sup> treatment of salt **7** to *N,N*-diisopropylaniline led to complete conversion to dimer **8** within 5 min. On the other hand, when salt **12** was treated to identical conditions, conversion to **13** and **14** took upwards of 7 hours, and when monitoring the reaction by  $^1\text{H}$  NMR, no signals were ever observed that could be attributed to ylide **12**<sup>(-)</sup>. We initially hypothesized that these slower conversion rates were the result of slower deprotonation, possibly due to an increase in sterics due to the close proximity of the proton to the methyl group of **12**. However, the steric hypothesis was disproven since switching to the less sterically demanding base, *N,N*-dimethylaniline slowed the consumption of **12** even more-so, consistent with the lower  $\text{p}K_{\text{a}}$  of *N,N*-dimethylaniline.<sup>9</sup> Likewise, *N,N*-dimethylaniline slowed down the conversion of salt **7** to dimer **8** to a rate more comparable with the rate that *N,N*-diisopropylaniline promotes the conversion of **12** to **13** and **14** (Scheme 4A). We thus treated a solution of **7** and DMAD (**16a**) in  $\text{CD}_3\text{CN}$  to *N,N*-dimethylaniline to assess whether greater trapping efficiency could be achieved with a slower deprotonation. However, when viewed at only partial conversion of salt **7** (15 min), dimer **8** remained the major product (Scheme 4B).



**Scheme 4. Effects of base on salt conversion and cycloaddition trapping efficiency.** (A) Conversion over time of salt **12** with *N,N*-diisopropylaniline and salt **7** with *N,N*-dimethylaniline. (B) Analysis of the ratio between cycloaddition and dimerization products for the reaction between **7** and DMAD (**16a**) when initiated by *N,N*-dimethylaniline, as observed at partial conversion.

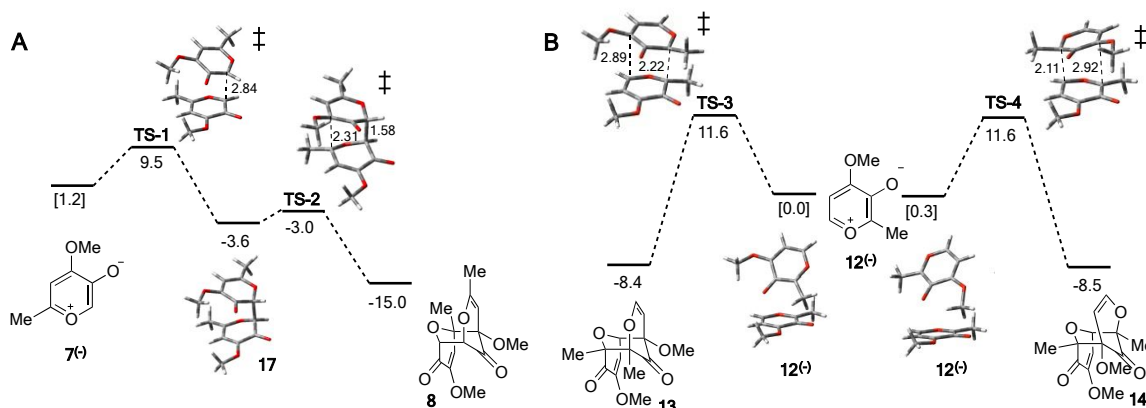
The above experimental results made it evident that the differences in DMAD (**16a**) trapping efficiency from salt **7** and **12** prior to dimerization could not be fully explained by simple differences in rates of deprotonation, and thus these differences might exist after the deprotonation step and involve relative reactivities of the ylides. Thus, we turned to DFT calculations to study the relative dimerization and cycloaddition reactions from **7<sup>(-)</sup>** and **12<sup>(-)</sup>**.

*DFT Calculations.* B3LYP/6-31G(d,p) calculations were employed here. Similar DFT calculations have been used to assess the tendency for compounds to dimerize,<sup>10</sup> and in cycloadditions of butadiene with oxidopyrylium ylides.<sup>11</sup> To explore the bimolecular pathways (**Scheme 5**), we have located structures on the potential energy surface (PES) for the dimerization of maltol **12<sup>(-)</sup>** and allomaltol **7<sup>(-)</sup>** oxidopyrylium ylides. Our calculations focused on the neutral forms of maltol and allomaltol oxidopyrylium ylides since these are expected to give rise to the dimers. Since **7<sup>(-)</sup>** and **12<sup>(-)</sup>** are structural isomers, their relative energies can be readily compared. The global minimum is the complex of **12<sup>(-)</sup>**.

**Scheme 5A** shows the formation of dimer **8** from the allomaltol-derived oxidopyrylium ylide **7<sup>(-)</sup>**, which proceeds through a step-wise process. This process involves an initial carbon-carbon bond formation *via* an aldol-like process between the  $\alpha$ -carbon of the embedded enolate of one ylide, and the more sterically unencumbered electrophilic carbon of the other. The reaction  $\Delta H^\ddagger$  is 8.3 kcal/mol (compared to **7<sup>(-)</sup>**), and leads to the second step, where a more sterically encumbered carbon creates the second carbon-carbon bond of dimer **8**. In the formation of dimer **8**, there is a methyl-methoxy gauche interaction, but it is a lower in energy likely due to the fact that it is an intermolecular process (**TS-2, Figure 1**). The formation of dimer **13** from maltol oxidopyrylium ylide **12<sup>(-)</sup>**, on the other hand, proceeds through an asynchronous concerted process (**Scheme 5B**). The dimerization of **12<sup>(-)</sup>** is higher in energy than the dimerization of **7<sup>(-)</sup>** due to an unfavorable methyl-methyl gauche interaction, producing a  $\sim 2$  kcal/mol higher transition state energy (i.e.,  $\Delta H^\ddagger$  of 11.6 kcal/mol) than that of **7<sup>(-)</sup>** (**TS-3, Figure 1**). An identical  $\Delta H^\ddagger$  of 11.6 kcal/mol energy barrier exists in the transition state to



dimer **14**. Even though sterics of a methoxy group are generally lower in energy than a methyl group, this specific methoxy-methyl gauche interaction appears to have added steric strain, where the methyl group of the methoxy extends over the incipient carbonyl group (TS-4, **Figure 1**). This explains why both dimers of **12<sup>(-)</sup>** are formed, in contrast to the selective [5 + 3] dimerization of **7<sup>(-)</sup>**.



**Scheme 5.** Computed potential energy surface of maltol and allomaltol oxidopyrylium ylides **7<sup>(-)</sup>** and **12<sup>(-)</sup>**. The computed potential surface uses two molecules of **7<sup>(-)</sup>** in A, and two molecules of **12<sup>(-)</sup>** in B.

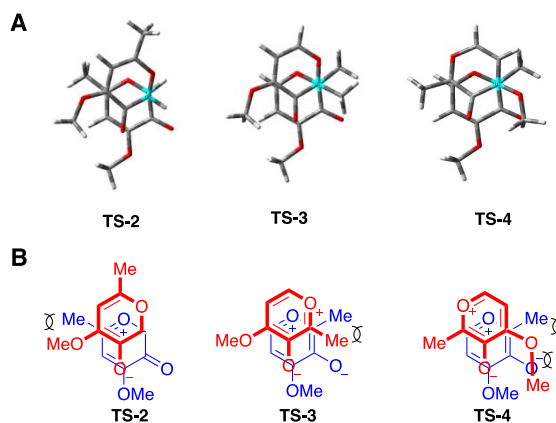
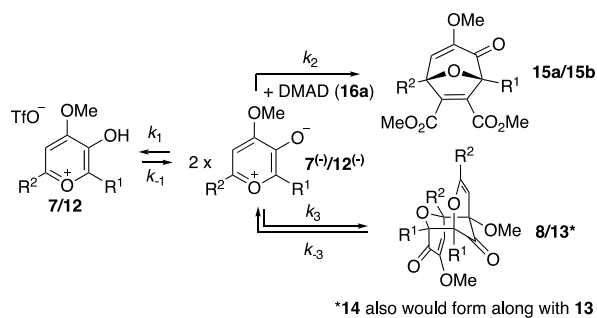


**Figure 1.** Top perspective of transition states to dimerization to highlight steric interactions. (A) Graphical perspective of the second bond forming reaction in production of **8**, (TS-2), and the concerted formation of dimer **13** and **14** demonstrating energetically costly steric interactions. (TS-3 and TS-4). (B) Transition state perspectives re-drawn and color coordinated for visual clarity.

The cycloaddition reactions between DMAD (**16a**) and either **7<sup>(-)</sup>** or **12<sup>(-)</sup>** were fairly analogous energetically, and each was predicted to proceed through a concerted, asynchronous pathway. The transition state between DMAD and **12<sup>(-)</sup>** was only slightly

1  
2  
3 favored over that between DMAD and  $7^{(-)}$  (11.7 vs. 12.9 kcal/mol, **Scheme 1S**, see SI  
4 section for details). Furthermore, cycloaddition products were thermodynamically  
5 favored over dimer products by approximately 40 kcal/mol in both cases, consistent with  
6 the observations that, with enough time and energy, all of the dimers investigated can be  
7 converted to their respective oxidopyrylium [5 + 2] cycloaddition products.  
8  
9

10  
11  
12  
13 *Kinetic Studies.* Kinetics experiments were carried out as a means to evaluate the  
14 relative transition state energy barriers for dimerization and cycloaddition processes.  
15 Drawing inspiration and precedence from classic kinetic studies on the reaction between  
16 dialkylborane dimers and alkenes by Brown *et al.*,<sup>12</sup> steady state approximation was  
17 employed to evaluate the reaction between oxidopyrylium dimers (**8/13/14**) and DMAD  
18 (**16a**) ( $8 + 16a \rightarrow 15b$  or  $13/14 + 16a \rightarrow 15a$ , **Scheme 6**). In this way, the kinetics are  
19 fixed on the key reactions of interest – namely, the [5 + 2] cycloaddition ( $k_2$ ) and  
20 dimerization/cycloreversion ( $k_3/k_{-3}$ ) (**Scheme 6**). Assuming the energy barrier for  
21 dimerization of  $12^{(-)}$  is higher than the energy barrier for the cycloaddition reaction with  
22 DMAD (**16a**) to an extent such that  $1/2k_2[16a] \gg k_3[12^{(-)}]$ , the reaction should exhibit  
23 first-order kinetics, as represented by the equation  $-d[13]/dt = k_1[13]$ . Conversely, if the  
24 cycloaddition step between  $7^{(-)}$  and DMAD (**16a**) is higher in energy than the  
25 dimerization of  $7^{(-)}$  such that  $1/2k_2[16a] \ll k_3[7^{(-)}]$ , then the reaction should exhibit  
26 three-halves-order kinetics, as represented by the equation  $-d[8]/dt = k_{3/2}[8]^{1/2}[16a]$ .  
27  
28  
29  
30  
31  
32  
33  
34  
35  
36  
37



48 **Scheme 6. Overview of competing cycloaddition and dimerization pathways from 7/12, also**  
49 **illustrating conversion of 8/13/14 to 15a/15b.**

50  
51  
52  
53 To evaluate the kinetics experimentally, conversion of **8** and **13** were monitored over  
54 time with an excess of DMAD (**16a**), and the resultant plots were evaluated for best fit  
55  
56  
57  
58  
59  
60

(Figure 2A).<sup>13</sup> Consistent with the anticipated kinetics, conversion of **8** fit best to half-order kinetics ( $[8]_t^{1/2}$  vs. time), whereas conversion of **13** fit best to first order kinetics ( $\ln[13]_t$  vs. time). We also carried out experiments in the inverse, with an excess of the dimers (Figure 2B). In the presence of dimer **13**, the rate of conversion of DMAD (**16a**) stayed consistent as the concentrations decreased, in line with 0<sup>th</sup> order kinetics. However, in the presence of dimer **8**, the rate changed as the concentration of DMAD (**16a**) changed, fitting best to 1<sup>st</sup> order kinetics ( $\ln[16a]_t$  vs. time). Experiments performed with **14** were also consistent with those performed with **13** (See supporting information). Thus, these studies provided experimental evidence that in the reaction between allomaltol-derived oxidopyrylium ylide **7**<sup>(-)</sup> and **16a**, dimer **8** is the kinetic product, helping explain the difficulty of intercepting **7**<sup>(-)</sup> with DMAD (**16a**). Conversely, the studies also provided experimental evidence that in the reaction between maltol-derived oxidopyrylium ylide **12**<sup>(-)</sup> and **16a**, cycloaddition product **15a** is the kinetic product, which explains why **12**<sup>(-)</sup> can be successfully intercepted with DMAD (**16a**).

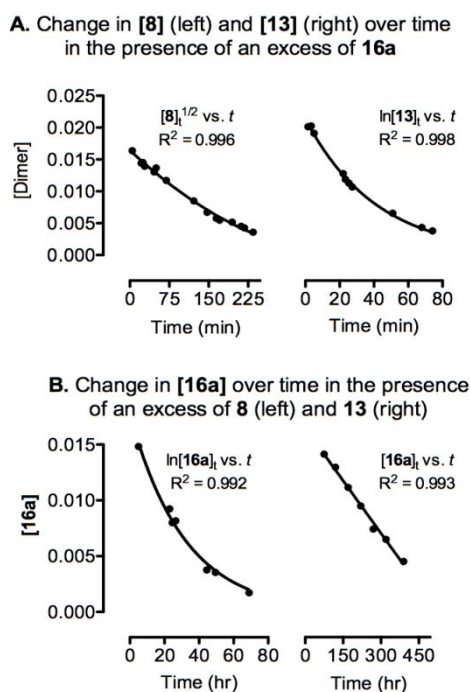
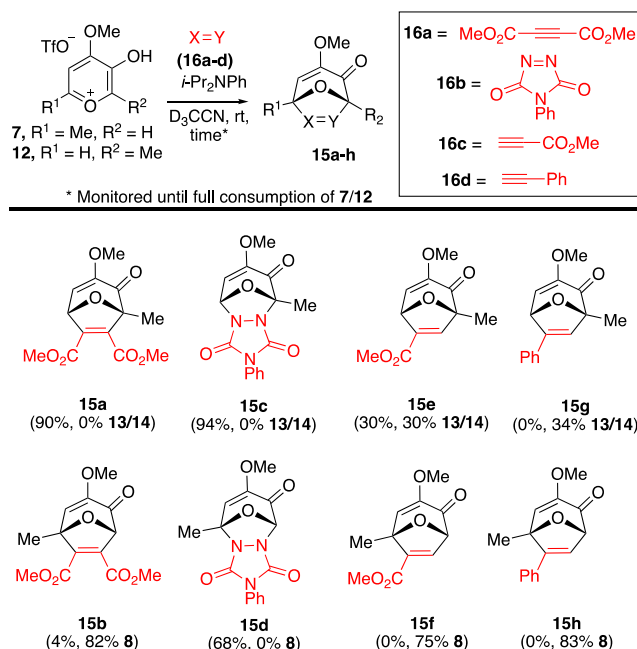


**Figure 2. Graphs from Kinetics Studies.** (A) The concentration of dimer **8** and **13** over time with an excess of **16a**. (B) **16a** in an excess of dimer **8** and **13**.

**Dipolarophile Dependence.** Both DFT calculations and kinetics experiments helped explain why DMAD (**16a**) is trapped more efficiently by **12**<sup>(-)</sup> than by **7**<sup>(-)</sup>. We next wanted to gauge how their relative trapping efficiency might extend to other dipolarophiles. For these studies, we added *N,N*-diisopropylaniline to a solution of CD<sub>3</sub>CN containing oxidopyrylium salts **7** and **12** and a panel of dipolarophiles of varying reactivity (**16a-d**), and monitored reaction progress by <sup>1</sup>H NMR (**Scheme 7**). Phenylacetylene (**16d**) is known to react more sluggishly with **7**<sup>(-)</sup> than DMAD (**16a**).<sup>4</sup> Transition state energy barriers were thus computed for the reaction of **16d** with **7**<sup>(-)</sup> to form **15g** ( $\Delta H^\ddagger = 16.3$  kcal/mol, **Scheme 2S**, see SI section for details) and for the reaction of **16d** with **12**<sup>(-)</sup> to form **15h** ( $\Delta H^\ddagger = 17.4$  kcal/mol, **Scheme 2S**, see SI section for details). As these energy barriers are each higher than their respective dimerization energy barriers, dimerization products should be the kinetic products in both instances. Consistent with this hypothesis, when *N,N*-diisopropylaniline was treated to a mixture of **16d** and either salt **7** or **12**, upon complete consumption of salts, only dimerization products were observed (see entry for products **15g/h**).



**Scheme 7. Products to dimer ratio upon oxidopyrylium ylide formation in the presence of a range of dipolarophiles.** Yields calculated by <sup>1</sup>H NMR integration using an internal standard following full consumption of salt.

For a more reactive dipolarophile, we turned to the highly electrophilic 4-phenyl-1,2,4-triazole-3,5-dione (PTAD, **16b**, see entry for products **15c/d**).<sup>14</sup> As anticipated, very low transition state energy barriers were calculated for the reaction between **16b** and both **7**<sup>(-)</sup> ( $\Delta H^\ddagger = 2.7$  kcal/mol) and **12**<sup>(-)</sup> ( $\Delta H^\ddagger = 3.1$  kcal/mol, **Scheme 3S**, see details in the SI section). As these barriers were each substantially lower than those of their respective dimerization reactions, **15c** and **15d** would both be expected to be the kinetic products. Consistent with this, when *N,N*-diisopropylaniline was treated to a mixture of **16b** and either salt **7** or **12**, no dimer was observed and the [5 + 2] cycloaddition products **15c** and **15d** predominated. These two sets of experiments demonstrated that with the more extremes on the dipolarophile reactivity spectra, trapping efficiency of the two salts are similar. However, when these experiments were performed with the more intermediately reactive dipolarophile, methyl propiolate (**16c**, see entry for products **15e/f**), differences in the trapping efficiencies of **7**<sup>(-)</sup> and **12**<sup>(-)</sup> returned. Specifically, when salt **7** was treated to the base in the presence of **16c**, only dimer **8** was observed, whereas significant amounts of product **15e** were observed in the analogous reaction with **12**.

*Mechanistic Interpretation and Implications.* Oxidopyrylium ylides **7**<sup>(-)</sup> and **12**<sup>(-)</sup> can undergo both [5 + 3] dimerization and [5 + 2] cycloaddition chemistry to generate dimers (**8**, **13**, **14**) or cycloaddition products (*i.e.*, **15a/b**), respectively. The dimerization to **8** and **13/14** is reversible and leads back to the ylides, which can then convert further to the thermodynamically stable oxidopyrylium cycloaddition products, **15a** and **15b**, when heated in the presence of DMAD (**16a**). Instead of the dimer reacting directly with the dipolarophile, the kinetic and computational results support a mechanism whereby dimer conversion to cycloaddition products proceeds through cycloreversion of the dimers to oxidopyrylium ylides followed by a cycloaddition reaction. Kinetics for these two reactions are different, however. Kinetics from the reaction from dimer **8** and DMAD (**16a**) is consistent with a mechanism wherein the transition state energy for [5 + 3] cycloreversion/dimerization is lower than that of the [5 + 2] cycloaddition reaction, and that from **13/14** consistent with one where the transition state for [5 + 3] cycloreversion/dimerization is higher in energy than the [5 + 2] cycloaddition step.

DFT studies were consistent with these trends, revealing that the transition state barrier for dimerization of **12<sup>(-)</sup>** is higher in energy than that of **7<sup>(-)</sup>** (**Scheme 5**), and thus **8** is the kinetic product relative to **15a**, whereas **15b** is the kinetic product relative to **13/14**. The DFT studies indicate that these energy differences are the result of unavoidable steric interactions in the transition state towards both dimer **13** and **14**, which alter the mechanism for the different dimerization reactions. The implications to these studies are that by positioning groups *ortho* to the oxide (e.g. **12<sup>(-)</sup>**), the transition state barrier towards dimerization can increase, and improve the success rate of trapping the ylide with a dipolarophile prior to self-dimerization. One could anticipate based upon these results that by increasing the size of these groups, rate of dimerization will be slowed even further and allow for even more efficient [5 + 2] trapping. Indeed, 2,4,6-triphenylpyrylium-3-oxide is one of the few oxidopyrylium ylides to ever be observed experimentally and does not dimerize,<sup>15</sup> which may be why it reacts with an extremely broad range of dipolarophiles.<sup>16</sup> In the current studies, dramatic differences in trapping efficiency were observed with DMAD (**16a**) and methyl propiolate (**16c**). However, the more reactive dipolarophile PTAD (**16b**) efficiently intercepted both ylides, whereas the less reactive dipolarophile phenylacetylene (**16d**) could not intercept either ylide. Thus, further structure-activity relationships with a broader range of both oxidopyrylium ylides and dipolarophiles is warranted.

## Conclusion

Synthetic, kinetic, and theoretical approaches have been developed to probe oxidopyrylium ylide reactivity in self-dimerization and cycloaddition reactions. We find the following results: (i) maltol- and allomaltol-derived oxidopyrylium salts serve as precursors to their corresponding oxidopyrylium ylides **7<sup>(-)</sup>** and **12<sup>(-)</sup>**, which themselves serve as intermediates in both self-dimerization or cycloaddition reactions; (ii) DFT calculations provide valuable insight on the dimerization mechanism of these two oxidopyrylium ylides where gauche methyl/methyl or methyl/methoxy interactions favor the dimerization in a kinetically not thermodynamically controlled fashion compared to the [5 + 2] cycloaddition selectivity; (iii) Kinetics for the reaction between dimethyl acetylenedicarboxylate (**16a**) and oxidopyrylium dimers suggest that the rate limiting

step with dimer **8** is the cycloaddition reaction; in contrast, the reaction with dimer **13** or **14** is consistent with a mechanism where the rate limiting step is the cycloreversion to ylide **12<sup>(-)</sup>**; (iv) While oxidopyrylium ylides **7<sup>(-)</sup>** and **12<sup>(-)</sup>** have very different trapping efficiency profiles with DMAD (**16a**) and methylpropiolate (**16c**), only cycloaddition products form in the presence of the more reactive PTAD (**16b**), and only dimers form in the presence of less reactive phenylacetylene (**16d**). These studies provide insight into how differences in structure of the oxidopyrylium ylides such as the placement of appendages can lead to significantly different reactivity behaviors. Future studies combining synthetic, kinetic, and theoretical studies across a broader range of oxidopyrylium ylides should further enhance our understanding of these systems, and help inform future synthetic strategies employing oxidopyrylium cycloaddition and dimerization reactions. For example, the decomposition of homodimers is a retro reaction of “masked” neutral oxidopyrylium ylide monomers, and is a base-free strategy that could be valuable for some reactions. In contrast to the reactivity of DMAD with dimers **8**, **13** and **14**, Hendrickson’s early work described how the reaction between the dimer of an unsubstituted 3-oxidopyrylium ylide and DMAD only forms trace products, even at 200 °C.<sup>2b</sup> Thus, there appear to be structural advantages to dimers **8**, **13**, and **14** that allow them to behave as oxidopyrylium ylide sources. It seems reasonable to hypothesize that the OMe plays an important role in this reactivity by both enhancing the nucleophilicity of the ylides and destabilizing the ground state of **8** and **14** through the gauche interactions it presents. Further studies are underway to assess the importance of the OMe group for efficient dimerization reversibility, and whether other oxidopyrylium ylide dimers without OMe groups may also behave as ylide sources. In other instances, dimerization may pose greater technical challenges, and knowledge of how to effectively trap out ylides prior to dimerization will be valuable.

## Experimental Section

**General Information.** All starting materials and reagents were purchased from commercially available sources and used without further purification, with the exception of CH<sub>2</sub>Cl<sub>2</sub>, which was purified on a solvent purification system prior to reactions. <sup>1</sup>H, and

<sup>13</sup>C NMR shifts were measured using the solvent residual peak as the internal standard and reported as follows: chemical shift, multiplicity (s = singlet, bs = broad singlet, d = doublet, t = triplet, dd = doublet of doublets, q = quartet, m = multiplet), coupling constant (Hz), integration. Infrared (IR) spectral bands are characterized as broad (br), strong (s), medium (m), and weak (w). Mass spectra were recorded on a spectrometer by the electrospray ionization (ESI) technique with a time-of-flight (TOF) mass analyzer. Microwave reactions were performed via the Biotage Initiator EXP US (manufacturer #: 355302)(external IR temperature sensor) in a sealed vessel. Where noted, reaction products were purified via silica gel chromatography using a Biotage Isolera Prime, with Biotage® SNAP Ultra 10 g or 25 g cartridges, in a solvent system of ethyl acetate (EtOAc) in hexane.

**Synthesis and Characterization of Maltol-Derived Oxidopyrylium Salt. 3-hydroxy-4-methoxy-2-methylpyrylium trifluoromethanesulfonate (12).** To a solution of maltol (**11**, 5g, 0.0396 mol) in CH<sub>2</sub>Cl<sub>2</sub> (10 mL) was added methyl trifluoromethanesulfonate (MeOTf, 6.5 mL, 0.0594 mol). The reaction was allowed to stir at reflux for 4 h, cooled to ambient temperature, and then evaporated under reduced pressure to yield **12** as solid white crystals (6.5 g, 54% yield), with a melting point range of 99-102 °C. **IR (thin film, KBr):** 3088 (w) 1634 (s) 1554 (w) 1497 (m) 1438 (w) 1258 (b) 1164 (s) 1069 (w) 1033 (s) 962 (w) 903 (w) 827 (w) 750 (b) 636 (s) cm<sup>-1</sup>. **<sup>1</sup>H NMR (400 MHz, CD<sub>3</sub>CN)** δ 8.80 (d, *J* = 5.2 Hz, 1H), 7.60 (d, *J* = 5.2 Hz, 1H), 4.31 (s, 3H), 2.68 (s, 3H). **<sup>13</sup>C{<sup>1</sup>H} NMR (101 MHz, CD<sub>3</sub>CN)** δ 168.8, 166.4, 161.2, 142.9, 108.5, 60.7, 16.3.

**Synthesis and Characterization of Maltol-Derived Oxidopyrylium Dimers (13) and (14).** In a round bottom flask, triflate salt **12** (0.1 g, 0.345 mmol, 1 eq), was suspended in CH<sub>2</sub>Cl<sub>2</sub> (3 mL, 0.1M). Triethylamine (96 µL, 0.690 mmol, 2 eq) was slowly added to the reaction mixture, at which time the solid slowly dissolved. The reaction mixture was allowed to stir for 2 h at room temperature, and was then quenched with saturated aqueous ammonium chloride (5 mL). The organic layer was isolated and the aqueous layer was extracted with CH<sub>2</sub>Cl<sub>2</sub> (3 x 10 mL). Combined organics were dried over Na<sub>2</sub>SO<sub>4</sub>, filtered, and concentrated under reduced pressure. The crude material was



purified by chromatography (Biotage Isolera Prime, SNAP 12 g silica gel, 18 cm x 1.8 cm, solvent gradient: 0-25% EtOAc in hexanes (500 mL). Two products were separated and product fractions were concentrated to yield **13** (22 mg, 0.0786, 45% yield) and **14** (12 mg, 0.0429, 25% yield), both isolated as white solids. **(±)-(1R,2S,6S,7R)-6,9-dimethoxy-1,2-dimethyl-3,11-dioxatricyclo[5.3.1.1<sup>2,6</sup>]dodeca-4,8-diene-10,12-dione (13)**. Mp: 129-132 °C.  $R_f$  = 0.14 in 20 % ethyl acetate in hexanes. **IR (ATR, ZnSe)** 3090 (w), 3002(w), 2941(br), 2834 (br), 1742(s), 1699(s), 1626(s), 1455(w), 1358(m), 1258(m), 1170(s), 1139(s), 1066(s), 1036(m), 914(m), 841(w), 789(w). **<sup>1</sup>H NMR (400 MHz, CDCl<sub>3</sub>)**  $\delta$  6.67 (d,  $J$  = 5.9 Hz, 1H), 6.01 (d,  $J$  = 5.1 Hz, 1H), 5.02 (d,  $J$  = 5.9 Hz, 1H), 4.49 (d,  $J$  = 5.1 Hz, 1H), 3.63 (s, 3H), 3.49 (s, 3H), 1.55 (s, 3H), 1.25 (s, 3H). **<sup>13</sup>C{<sup>1</sup>H} NMR (101 MHz, CDCl<sub>3</sub>)**  $\delta$  199.5, 188.8, 149.9, 148.2, 113.0, 100.5, 92.4, 87.6, 86.3, 77.4, 55.5, 54.1, 17.3, 14.7. **HRMS (ESI-TOF)**  $m/z$ : [M+H]<sup>+</sup> calc'd for C<sub>7</sub>H<sub>9</sub>O<sub>3</sub><sup>+</sup>: 141.0473 Found: 141.0561. **(±)-(1R,2R,6R,7R)-6,9-dimethoxy-2,7-dimethyl-3,11-dioxatricyclo[5.3.1.1<sup>2,6</sup>]dodeca-4,9-diene-8,12-dione (14)**. Mp: 159-159 °C.  $R_f$  = 0.14 in 25 % ethyl acetate. **IR (ATR, ZnSe)** 3090 (w), 3002(w), 2941(br), 2834 (br), 1742(s), 1699(s), 1626(s), 1455(w), 1358(m), 1258(m), 1170(s), 1139(s), 1066(s), 1036(m), 914(m), 841(w), 789(w). **<sup>1</sup>H NMR (400 MHz, CDCl<sub>3</sub>)**  $\delta$  6.69 (d,  $J$  = 6.0 Hz, 1H), 5.64 (d,  $J$  = 5.2 Hz, 1H), 4.92 (d,  $J$  = 6.0 Hz, 1H), 4.74 (d,  $J$  = 5.2 Hz, 1H), 3.60 (s, 3H), 3.43 (s, 3H), 1.45 (s, 3H), 1.39 (s, 3H). **<sup>13</sup>C{<sup>1</sup>H} NMR (101 MHz, CDCl<sub>3</sub>)**  $\delta$  199.3, 188.5, 150.7, 148.3, 109.0, 98.3, 89.7, 87.8, 86.0, 80.0, 55.4, 54.5, 17.1, 17.0. **HRMS (ESI-TOF)**  $m/z$ : [M+H]<sup>+</sup> calc'd for C<sub>7</sub>H<sub>9</sub>O<sub>3</sub><sup>+</sup>: 141.0473 Found: 141.0838. *Stereochemistry of 13 and 14 were determined by X-ray crystal analysis. See X-ray section, below, for details.*

#### Synthesis of New Oxidopyrylium [5 + 2] Cycloadducts for Characterization.

*Cycloadducts 15b, 15f and 15h were synthesized previously.<sup>4</sup> Compounds 15a, 15c, 15d, 15e, and 15g were synthesized as follows to provide characterization data in support of <sup>1</sup>H NMR yields described in Scheme 7.*

**(±)-Dimethyl (1S,5S)-3-methoxy-5-methyl-4-oxo-8-oxabicyclo[3.2.1]octa-2,6-diene-6,7-dicarboxylate (15a)**. To a solution of **13/14** (20 mg, 0.0714mmol, 1 eq) in CDCl<sub>3</sub>

(1 mL, 0.9 M) was added dimethyl acetylenedicarboxylate (**16a**, 100  $\mu$ L, 0.814 mmol, 11 eq). The reaction was subjected to microwave irradiation at 150  $^{\circ}$ C for 2 h, and immediately purified by chromatography (Biotage Isolera Prime, SiliCycle SiliaSep 25 g silica gel, 40-63  $\mu$ m 60  $\text{\AA}$ , solvent gradient: 0-25% EtOAc in hexanes (500 mL)). Product fractions were concentrated *en vacuo* to yield **15a** as a pale, yellow oil (38 mg, 95% yield).  $R_f$  = 0.53 in 25% ethyl acetate. **IR (thin film, KBr):** 2956 (w), 2843 (w), 1716 (s), 1654 (w), 1614 (m), 1438 (m), 1379 (w), 1281 (b), 1146 (w), 1069 (s), 1005 (m), 933 (w), 902 (w), 878 (w), 847 (w), 812 (w), 787 (w), 766 (w), 700 (w), 6309 (w)  $\text{cm}^{-1}$ .  **$^1\text{H}$  NMR (400 MHz,  $\text{CDCl}_3$ )**  $\delta$  6.15 (d,  $J$  = 4.9 Hz, 1H), 5.39 (d,  $J$  = 4.9 Hz, 1H), 3.79 (d,  $J$  = 6.4 Hz, 6H), 3.56 (s, 3H), 1.59 (s, 3H).  **$^{13}\text{C}\{^1\text{H}\}$  NMR (101 MHz,  $\text{CDCl}_3$ )**  $\delta$  188.2, 163.1, 162.1, 146.5, 146.4, 143.1, 114.4, 94.0, 78.2, 55.1, 52.8, 52.8, 16.2. **HRMS (ESI-TOF)  $m/z$ :**  $[\text{M}+\text{H}]^+$  calc'd for  $\text{C}_{13}\text{H}_{15}\text{O}_7^+$ : 283.0812 Found: 283.0817 ( $\pm$ )-(5*R*,9*S*)-7-methoxy-5-methyl-2-phenyl-1*H*,5*H*-5,9-epoxy[1,2,4]triazolo[1,2-*a*][1,2]diazepine-1,3,6(2*H*,9*H*)-trione (**15c**). To a solution of **12** (50 mg, 0.172 mmol, 1 eq) and 4-Phenyl-1,2,4-triazole-3,5-dione (**16b**, 60 mg, 0.344 mmol, 2 eq) in  $\text{CD}_3\text{CN}$  (600  $\mu$ L, 0.3M) was added *N,N*-diisopropylaniline (29  $\mu$ L, 0.2068 mmol, 1.2 eq). The reaction stirred for 5 minutes and was then immediately purified by chromatography (Biotage Isolera Prime, SiliCycle, SiliaSep 25 g silica gel column, 40-63  $\mu$ m 60  $\text{\AA}$ , solvent gradient: 0-25% EtOAc in hexanes (500 mL)). Product fractions were concentrated *en vacuo* to yield **12** as a white solid (39 mg, 72% yield). Mp: 65-70  $^{\circ}$ C.  $R_f$  = 0.50 in 25% in ethyl acetate. **IR (thin film, KBr):** 3429 (br), 1731 (s), 1633 (w), 1498 (w), 1399 (m), 1363 (w), 1232 (w), 1148 (w), 1075 (m), 778 (w), 690 (w)  $\text{cm}^{-1}$ .  **$^1\text{H}$  NMR (400 MHz,  $\text{CDCl}_3$ )**  $\delta$  7.51 – 7.38 (m, 5H), 6.34 (d,  $J$  = 5.0 Hz, 1H), 6.11 (d,  $J$  = 5.0 Hz, 1H), 3.70 (s, 3H), 1.96 (s, 3H).  **$^{13}\text{C}\{^1\text{H}\}$  NMR (101 MHz,  $\text{CDCl}_3$ )**  $\delta$  182.2, 156.5, 154.87, 150.9, 130.9, 129.5, 129.1, 125.6, 109.8, 96.8, 83.4, 55.9, 15.2. **HRMS (ESI-TOF)  $m/z$ :**  $[\text{M}+\text{H}]^+$  calc'd for  $\text{C}_{15}\text{H}_{14}\text{N}_3\text{O}_5^+$ : 316.0928 Found: 316.0928.

**Synthesis of (5*R*,9*S*)-7-methoxy-9-methyl-2-phenyl-1*H*,5*H*-5,9-epoxy[1,2,4]triazolo[1,2-*a*][1,2]diazepine-1,3,6(2*H*,9*H*)-trione (**15d**) in the presence of excess salt\*:** To a mixture of oxidopyrylium salt **12** (20 mg, 0.0689 mmol) and 4-phenyl-1,2,4-triazoline-3,5-dione (**16b**, 8 mg 0.0457 mmol) in DCM (1 mL, 0.0457 M)

was added triethylamine (12  $\mu$ L, 0.0860 mmol). The reaction was stirred for 5 minutes at room temperature and subsequently washed with aqueous ammonium chloride (3 x 3 mL). The organic layer was isolated and the aqueous layer was extracted with  $\text{CH}_2\text{Cl}_2$  (3 x 5 mL). Combined organic layers were dried over  $\text{Na}_2\text{SO}_4$ , filtered and concentrated under reduced pressure to yield a mixture of dimer **8**, cycloadduct **15d**, and PTAD (**16b**). **15d** is unstable to chromatography and attempts at crystallization were unsuccessful. It was thus characterized as a mixture of the three. See supporting information for further details.  **$^1\text{H}$  NMR (400 MHz,  $\text{CD}_3\text{CN}$ )**  $\delta$  7.59 – 7.35 (m, Ar)\*, 6.28 (s, 1H), 5.86 (s, 1H), 3.66 (s, 3H), 2.07 (s, 3H).  **$^{13}\text{C}\{^1\text{H}\}$  NMR (101 MHz,  $\text{CDCl}_3$ )**  $\delta$  182.5, 157.3, 155.8, 150.5, 125-135 (Ar)\*, 116.6, 89.9, 56.5, 55.3, 21.1. \*Aromatic regions undefined due to presence of PTAD overlapping in the aromatic region. **HRMS (ESI-TOF)  $m/z$ :  $[\text{M}+\text{H}]^+$**  calc'd for  $\text{C}_{15}\text{H}_{14}\text{N}_3\text{O}_5^+$ : 316.0928 Found: 316.0928.

**( $\pm$ )-Methyl (1*S*,5*S*)-3-methoxy-1-methyl-2-oxo-8-oxabicyclo[3.2.1]octa-3,6-diene-6-carboxylate (**15e**).** To a solution of **14** (25 mg, 0.0893 mmol, 1 eq) in  $\text{CDCl}_3$  (1 mL, 0.9M) was added methylpropiolate (**16c**, 80  $\mu$ L, 0.893 mmol, 10 eq). The reaction was subjected to microwave irradiation at 100  $^\circ\text{C}$  for 2 h and then purified by chromatography (Biotage Isolera Prime, SiliCycle SiliaSep 25 g silica gel column, 40-63  $\mu\text{m}$  60  $\text{\AA}$ , solvent gradient: 0-25% EtOAc in hexanes (500 mL)). Product fractions were concentrated *en vacuo* to yield **15e** as a yellow oil (18 mg, 60% yield).  $R_f$  = 0.20 in 25% ethyl acetate. **IR (thin film, KBr):** 3448 (br), 2956 (w), 2358 (w), 1716 (s), 1654 (w), 1614 (m), 1438 (m), 1336 (m), 1379 (w), 1227 (w), 1281 (br), 1146 (w), 1069 (s), 1033 (m), 933 (w), 902 (w), 878 (w), 847 (w), 812 (w)  $\text{cm}^{-1}$ .  **$^1\text{H}$  NMR (400 MHz,  $\text{CDCl}_3$ )**  $\delta$  6.88 (s, 1H), 6.22 (d,  $J$  = 4.9 Hz, 1H), 5.41 (d,  $J$  = 4.9 Hz, 1H), 3.81 (s, 3H), 3.57 (s, 3H), 1.59 (s, 3H).  **$^{13}\text{C}\{^1\text{H}\}$  NMR (101 MHz,  $\text{CDCl}_3$ )**  $\delta$  190.6, 163.1, 148.2, 146.5, 142.2, 115.6, 93.5, 78.1, 55.0, 52.4, 17.1. **HRMS (ESI-TOF)  $m/z$ :  $[\text{M}+\text{H}]^+$**  calc'd for  $\text{C}_{11}\text{H}_{13}\text{O}_5^+$ : 225.0757 Found: 225.0751.

**( $\pm$ )-(1*S*,5*S*)-3-methoxy-1-methyl-6-phenyl-8-oxabicyclo[3.2.1]octa-3,6-dien-2-one (**15g**).** To a solution of **14** (25 mg, 0.0893 mmol, 1 eq) in  $\text{CDCl}_3$  (1 mL, 0.9 M) was added phenylacetylene (**16d**, 100  $\mu$ L, 0.911 mmol, 11 eq). The reaction was

subjected to microwave irradiation at 120 °C for 8 h and then purified by chromatography (Biotage Isolera Prime, SiliCycle SiliaSep 25 g silica gel column, 40-63  $\mu\text{m}$  60 Å, solvent gradient: 0-25% EtOAc in hexanes (500 mL)). Product fractions were concentrated *en vacuo* to yield **14** as a yellow oil (7 mg, 16% yield).  $R_f$  = 0.13 in 25 % in ethyl acetate. **IR (thin film, KBr):** 3446 (br) 2933 (w) 1705 (s) 1614 (m) 1446 (w) 1343 (w) 1242 (w) 1063 (br) 905 (w) 852 (w) 691 (w) 649 (w)  $\text{cm}^{-1}$ .  **$^1\text{H}$  NMR (400 MHz,  $\text{CDCl}_3$ )**  $\delta$  7.42 – 7.35 (m, 5H), 6.30 (d,  $J$  = 4.9 Hz, 1H), 6.27 (s, 1H), 5.58 (d,  $J$  = 4.8 Hz, 1H), 3.55 (s, 3H), 1.63 (s, 3H).  **$^{13}\text{C}\{^1\text{H}\}$  NMR (101 MHz,  $\text{CDCl}_3$ )**  $\delta$  191.6, 155.8, 147.4, 131.9, 129.4, 129.1, 126.0, 124.0, 114.9, 93.1, 79.1, 55.0, 17.6. **HRMS (ESI-TOF)  $m/z$ :**  $[\text{M}+\text{H}]^+$  calc'd for  $\text{C}_{15}\text{H}_{15}\text{O}_3^+$ : 243.1016 Found: 243.1001.

#### Evaluation of Product *versus* Dimer Upon Full Conversion of Oxidopyrylium Salt.

In a small vial, salt (**7** or **12**) (5mg, 0.0172 mmol, 1 eq), alkyne (**16a-d**) (0.172 mmol, 10 eq) in 600  $\mu\text{L}$  of  $\text{CD}_3\text{CN}$  was added  $N,N$ -diisopropylaniline (4  $\mu\text{L}$ , 0.0207 mmol, 1.2 eq). The reaction was monitored over time by  $^1\text{H}$  NMR, and yields were calculated using  $^1\text{H}$  NMR integration based upon known amount of 3,5-ditertbutyltoluene standard in the reaction mixture. For conversion to known compounds **15b**, **15f**, **15h**, and **8**,  $^1\text{H}$  NMR of reactions were compared to literature spectra.<sup>4</sup>

**Rate Studies.** All rate studies were conducted in Wilmad® low pressure/vacuum NMR tube where concentrations of substrates were determined via known amount of added internal NMR standard, 3,5-Di-tert-butyltoluene. For conversion to known compound **15b**,  $^1\text{H}$  NMR spectra were compared to literature spectra.<sup>4</sup> All experiments were run at least twice to obtain consistent data sets.

**General procedure for excess of 16a with dimers 8, 13, and 14 separately:** To dimer (**8**, **13**, or **14**) (3 mg, 0.01 mmol) in 600  $\mu\text{L}$  of deuterated toluene was added **16a** (26.5  $\mu\text{L}$ , 0.2 mmol, 20 eq). The reaction was heated in an oil bath (100 °C for

dimers **13** and **14**, 70 °C for dimer **8**) and monitored to near completion via internal NMR standard (3,5-di-tert-butyltoluene).

**General procedure for excess of dimers **8**,<sup>4</sup>**13**, and **14** separately with **16a**:** To dimer (**8**, **13**, or **14**) (15 mg, 0.05 mmol) in 600  $\mu$ L of deuterated toluene was added **16a** (1.3  $\mu$ L, 0.01 mmol). The reaction was heated in an oil bath (100 °C for dimers **13** and **14**, 70 °C for dimer **8**) and monitored to near completion via internal NMR standard (3,5-di-tert-butyltoluene).

**Computational Methods.** Optimizations, frequency calculations, the intrinsic reaction coordinate calculations were performed with Gaussian 09 (revision D.01)<sup>17</sup> at the  $\square$ 3LYP/6-31G(d,p) level of theory<sup>18</sup> and visualized with Gaussview 5.0.<sup>19</sup> These calculations yielded results in reasonably good agreement with experiment. The energetics are reported as the thermal enthalpies. For the potential energy surface (PES) in Scheme 5, frequency calculations established the nature of the stationary point obtained. Vibrational analyses showed that **TS-1**—**TS-4** species were transition structures, while **7**<sup>(-)</sup>, **8**, **12**<sup>(-)</sup>, **13**, and **17** minima. The intrinsic reaction coordinate (IRC)<sup>20</sup> calculations were used to verify the transition structures **TS-1**—**TS-4**.

**X-Ray.** The structures of **8**, **13**, and **14** are the first to be determined for these tricyclic heterocycles, and they confirm the proposed structures. Crystals were grown using vapor diffusion technique, using minimal ethyl acetate to solubilize dimers and hexanes as the outer solvent. The crystals of **13** and **14** appeared to be split crystals, most likely with more than two domains, giving rise to relatively high residuals due to overlapping peaks and in addition **13** was not strongly diffracting. The X-ray intensity data were measured on a Bruker Smart Breeze CCD system equipped with a graphite monochromator at 100(2) K, cooled by an Oxford Cryosystems 700 Series Cryostream. A total of 1464 frames were collected and were integrated with the Bruker SAINT software package, using a narrow-frame algorithm. Data were corrected for absorption effects using the multi-scan method (SADABS or TWINABS). The structures were solved and refined

using the Bruker SHELXTL Software Package. All data and methods may be found in the cif files included in the Supporting Information. Briefly, refinement of **8** was routine and **13** was refined as a 2-component twin. Compound **14** had to be refined as a 2-component twin but the second domain refined to just 2%, and it also exhibited a ~1:1 disorder for molecule 2 of the two in the asymmetric unit, for one methoxy methyl and one methyl group.

Cambridge Crystallographic Data Centre deposition numbers for **8**, **13**, and **14**: CCDC 1935838, 1935839, and 1935840. The data can be obtained free from Cambridge Crystallographic Data Centre via <https://www.ccdc.cam.ac.uk/structures/>

**Acknowledgment.** LPB, AKG, DMS, and RPM acknowledge support from the National Institutes of Health (SC1GM111158). EMG acknowledges support from the donors of the Petroleum Research Fund of the American Chemical Society. AG acknowledges support from the National Science Foundation (CHE-1856765). This work used Comet, the Extreme Science and Engineering Discovery Environment (XSEDE) cluster at the San Diego Supercomputer Center, which is supported by National Science Foundation grant number ACI-1548562 through allocation CHE-180060. We also thank PSC-CUNY for funding.

**Supplementary Data.** <sup>1</sup>H and <sup>13</sup>C NMR spectra of all new compounds, a discussion on characterization of **15d** as a mixture, including <sup>1</sup>H and <sup>13</sup>C NMR data of PTAD (**16d**) and dimer **8**, graphs used to determine kinetic rate data, DFT computed data, and X-ray data for **8**, **13**, and **14**. This material is available free of charge via the Internet at <http://pubs.acs.org>.

---

<sup>1</sup> For some lead examples, see: (a) Hendrickson, J.B.; Farina, J. S. A New 7-Ring Cycloaddition Reaction, *J. Org. Chem.* **1980**, *45*, 3359-3361. (b) Sammes, P. G.; Street, L. J. Intramolecular Cycloadditions with Oxidopyrylium Ylides. *J. Chem. Soc., Chem. Commun.* 1982, 1056-1057. (c) Mei, G.; Liu, X.; Quao, C.; Chen, W.; Li, C.-C. Type II Intramolecular [5 + 2] Cycloaddition: Facile Synthesis of ighly Functionalized Bridged Ring Systems. *Angew. Chem. Int. Ed.* **2015**, *54*, 1754-1758. (d) Liu, J. -Y.; Wu, J.-L.; Fan, J.-H.; Yan, X.; Mei, G.; Li, C.-C. Asymmetric Total Synthesis of Cyclotrinol. *J. Am. Chem. Soc.* **2018**, *140*, 5365-5369. (e) Liu, X.; Liu, J.-Y.; Wu, J.-L.; Huang, G.-C.; Liang, R.; Chung, L.-W.; Li, C.-C. Asymetric Total

- Synthesis of Cerorubenic Acid-III. *J. Am. Chem. Soc.* **2019**, *141*, 2872-2877. (f) Nicolaou, K. C.; Kang, Q.; Ng, S. Y.; Chen, D. Y.-K. Total synthesis of englerin A. *J. Am. Chem. Soc.* **2010**, *132*, 8219-8222. (g) Snider, B.B.; Wu, X.; Nakamura, S.; Hashimoto, S. A short biomimetic synthesis of (±)-polygalolides A and B. *Org. Lett.* **2007**, *9*, 873-874. (h) Wender, P. A.; Mascareñas, J. L. Studies on tumor promoters. 11. A new [5+2] cycloaddition method and its application to the synthesis of BC ring precursors of phorboids. *J. Org. Chem.* **1991**, *56*, 6267-6269. (i) Zhao, C.; Glazier, D. A.; Yang, D.; Yin, D.; Guzel, I. A.; Aristov, M. M.; Liu, P.; Tang, W. Intermolecular regio- and stereoselective hetero-[5 + 2] cycloaddition of oxidopyrylium ylides and cyclic imines. *Angew. Chem. Int. Ed.* **2019**, *58*, 887-891. (j) Tchabanenko, K.; McIntyre, P.; Malone, J. F. Rapid annulation of tropolone units via a pyrylium ylide 1,3-dipolar cycloaddition reaction. *Tetrahedron Letters*, **2010**, *51*, 86-88. (k) Adlington, R. M.; Baldwin, J. E.; Mayweg, A. V. W.; Pritchard, G. J. Biomimetic cycloaddition approach to tropolone natural products via an ortho-quinone methide. *Org. Lett.* **2002**, *4*, 3009-3011. (l) Suga, H.; Iwai, T.; Shimizu, M.; Takahashi, K.; Toda, Y. Efficient generation of an oxidopyrylium ylide using a Pd catalyst and its [5+2] cycloadditions with several dipolarophiles. *Chem. Comm.* **2018**, *54*, 1109-1112. (m) Magnus, P.; Shen, L. Stereoselective synthesis of the “cyathin” diterpene skeleton via an intramolecular pyrylium ylide-alkene cyclization. *Tetrahedron* **1999**, *55*, 3553-3560. (n) Woodall, E. L.; Simanis, J. A.; Hamaker, C. G.; Goodell, J. R.; Mitchell, T. A. Unique Reactivity of anti- and syn-Acetoxypyranones en Route to Oxidopyrylium Intermediates Leading to a Cascade Process. *Org. Lett.* **2013**, *15*, 3270-3273. For reviews, see: (o) Bejcek, L. P.; Murelli, R. P. Oxidopyrylium [5 + 2] Cycloaddition Chemistry: Historical Perspective and Recent Advances (2008-2018). *Tetrahedron*, **2018**, *74*, 2501-2521. (p) Singh, V.; Krishna, U. M.; Vikrant, Trivedi, G. K. Cycloaddition of Oxidopyrylium Species in Organic Synthesis. *Tetrahedron* **2008**, *64*, 3405-3428. (q) Ylijoki, K. E. O.; Stryker, J. M. [5 + 2] Cycloaddition Reactions in Organic and Natural Product Synthesis. *Chem. Rev.* **2013**, *113*, 2244-2266.
- <sup>2</sup> (a) Lee, H.-Y.; Kim, H.-Y.; Kim, B. G.; Kee, J. M. The Stereoselective Dimerization Reaction of Oxidopyrylium Ions. *Synthesis*, **2007**, *15*, 2360-2364. (b) Hendrickson, J. B.; Farina, J. S. A simple synthesis of 8- and 10-membered carbocyclic rings. *J. Org. Chem.* **1980**, *45*, 3361-3363.
- <sup>3</sup> Wender, P. A.; Mascareñas, J. L. Preparation and Cycloadditions of a 4-Methoxy-3-oxidopyrylium Ylide: A Reagent for the Synthesis of Highly Substituted 7-Membered Rings and Tetrahydrofurans. *Tetrahedron Lett.* **1992**, *33*, 2115-2118
- <sup>4</sup> Meck, C.; Mohd, N.; Murelli, R. P. An Oxidopyrylium Cyclization/ Ring-Opening Route to Polysubstituted  $\alpha$ -Hydroxytropolones. *Org. Lett.* **2012**, *14*, 5988-5991.
- <sup>5</sup> D'Erasmio, M. P.; Murelli, R. P. Discovery and Development of a 3-Component Oxidopyrylium [5 + 2] Cycloaddition Reaction. *J. Org. Chem.* **2018**, *83*, 1478-1485.
- <sup>6</sup> (a) D'Erasmio, M. P.; Masaoka, T.; Wilson, J. A.; Hunte, E. M. Jr.; Beutler, J. A.; Le Grice, S. F. J.; Murelli, R. P. D'Erasmio, M. P.; Masaoka, T.; Wilson, J. A.; Hunte, E. M. Jr.; Beutler, J. A.; Le Grice, S. F. J.; Murelli, R. P. Traceless Solid-Phase  $\alpha$ -Hydroxytropolone Synthesis. *MedChemComm.* **2016**, *9*, 1789-92. (b) Fuhr, K. N.; Hirsch, D. R.; Murelli, R. P.; Brenner-Moyer, S. E. Catalytic Enantioselective Intermolecular [5 + 2] Dipolar Cycloadditions of a 3-Hydroxy-4-Pyrone-Derived Oxidopyrylium Ylide. *Org. Lett.*, **2017**, *19*, 6356-6359.
- <sup>7</sup> Hirsch, D. R.; Schiavone, D. V.; Berkowitz, A. J.; Morrison, L. A.; Masaoka, T.; Wilson, J. A.; Lomonosova, E.; Zhao, H.; Patel, B. S.; Dalta, S. H.; Majidi, S. J.; Pal, R.; K.; Gallicchio, E.; Tang, L.; Tavis, J. E.; Le Grice, S. F. J.; Beutler, J. A.; Murelli, R. P. Synthesis and Biological Assessment of 3,7-Dihydroxytropolones. *Org. Biomol. Chem.* **2018**, *16*, 62-69.
- <sup>8</sup> (a) Mei, G.; Yuan, H.; Gu, Y.; Chen, W.; Chung, L. W.; Li, C.-C. Dearomative Indole [5 + 2] Cycloaddition Reactions: Stereoselective Synthesis of Highly Functionalized Cyclohepta[b]indoles. *Angew. Chem. Int. Ed.* **2014**, *126*, 11051-11055. (b) For studies on cycloaddition chemistry directly from salt **12**, see: Mascareñas, J. L.; Perez, I.; Rumbo, A.; Castedo, L. A New [5 + 2] Annulation Method for the Synthesis of 8-oxabicyclo[3.2.1]octanes from Pyrones. *Synlett*, **1997**, *1*, 81-82.
- <sup>9</sup> Measured  $pK_a$  of *N,N*-diisopropylaniline and *N,N*-dimethylaniline are 7.4 and 5.12, respectively. See: Adams, D. J.; Johns, B.; Vedernikov, A. N. Methyl Transfer Reactivity of Pentachloromethylplatinate(IV) Anion with a Series of *N*-Nucleophiles. *J. Organomet. Chem.* **2019**, *880*, 22-28.
- <sup>10</sup> (a) Voloshchuk, T.; Farina, N. S.; Wauchope, O. R.; Kiprowska, M.; Haberfield, P.; Greer, A. Molecular Bilateral Symmetry of Natural Products: Prediction of Selectivity of Dimeric Molecules by Density

- Functional Theory and Semiempirical Calculations. *J. Nat. Prod.* **2004**, *67*, 1141-1146. (b) Greer, A.; Wauchope, O. R.; Farina, N. S.; Haberfield, P.; Liebman, J. F. Paradigms and Paradoxes: Mechanisms for Possible Enhanced Biological Activity of Bilaterally Symmetrical Chemicals. *Struct. Chem.* **2006**, *17*, 347-350.
- <sup>11</sup> (a) Burns, J. M.; Boittier, E. D. Pathway Bifurcation in the [4 + 3]/[5 + 2]-Cycloaddition of Butadiene and Oxidopyrylium Ylides: The Significance of Molecular Orbital Isosymmetry. *J. Org. Chem.* **2019**, *84*, 5997-6005. (b) Kaufman, R. H.; Law, M. C.; Simanis, J. A.; Woodall, E. L.; Zwick, C. R., III; Wedler, H. B.; Wendelboe, P.; Hamaker, C. G.; Goodell, J. R.; Tantillo, D. J.; Mitchell, T. A. Oxidopyrylium-Alkene [5 + 2] Cycloaddition Conjugate Addition Cascade (C3) Sequences: Scope, Limitation, and Computational Investigations. *J. Org. Chem.* **2018**, *83*, 9818-9838. (c) Kuthanapillil, J. M.; Nijamudheen, A.; Joseph, N.; Prakash, P.; Suresh, E.; Datta, A.; Radhakrishnan, K. V. Cycloaddition of Pentafulvenes with 3-Oxidopyrylium Betaine: Experimental and Theoretical Investigations. *Tetrahedron*, **2013**, *69*, 9751-9760.
- <sup>12</sup> Brown, H. C.; Wang, K. K.; Scouten, C. G. Hydroboration Kinetics: Unusual Kinetics for the Reaction of 9-Borabicyclo[3.3.1]nonane with Representative Alkenes. *Proc. Nat. Acad. Sci. USA*, **1980**, *77*, 698-702.
- <sup>13</sup> Meek, S. J.; Pitman, C. L.; Miller, A. J. M. Deducing Reaction Mechanism: A Guide for Students, Researchers, and Instructors. *J. Chem. Educ.* **2016**, *93*, 275-286.
- <sup>14</sup> Adam, W.; De Lucchi, O.; Hill, K. Reaction of 4 - phenyl - 1,2,4 - triazoline - 3,5 - dione (PTAD) with Bicyclic Monoterpenes. *Eur. J. Inorg. Chem.* **1982**, *115*, 1982-1989.
- <sup>15</sup> Suld, G.; Price, C. C. Thiabenzene. I. 1,2,4,6-Tetraphenylthiabenzene. A New Conjugated Ring System. *J. Am. Chem. Soc.* **1961**, *83*, 1770-1771.
- <sup>16</sup> (a) Potts, K. T.; Elliott, A. J.; Sorm, M. Mesoionic Compounds. XVI. 1,4-Dipolar Type Cycloaddition Reactions Utilizing Pyrimidinium Betaines. *J. Org. Chem.* **1972**, *37*, 1422-1425. (b) Wasserman, H. H.; Pavia, D. L. Reaction of 2,4,6-Triphenylpyrylium 3-Oxide with Oxygen. *J. Chem. Soc. D.* **1970**, 1459-1460.
- <sup>17</sup> Frisch, M. J.; Trucks, G. W.; Schlegel, H. B.; Scuseria, G. E.; Robb, M. A.; Scalmani, J. G.; Barone, V.; Mennucci, B.; Petersson, G. A.; Caricato, H. M.; Li, X.; Hratchian, H. P.; Izmaylov, A. F.; Zheng, J. G.; Sonnenberg, J. L.; Hada, M.; Ehara, M.; Fukuda, K. R.; Hasegawa, J.; Ishida, M.; Nakajima, T.; Honda, Y.; Nakai, O. H.; Vreven, T.; Montgomery, J. A.; Peralta, J. E.; Bearpark, F. M.; Heyd, J. J.; Brothers, E.; Kudin, K. N.; Staroverov, V. N.; Kobayashi, R.; Normand, J.; Raghavachari, K.; Rendell, A.; Burant, J. C.; Iyengar, S. S.; Tomasi, J.; Cossi, M.; Millam, N. M.; Klene, M.; Knox, J. E.; Cross, J. B.; Bakken, V.; Jaramillo, C. A.; Gomperts, R.; Stratmann, R. E.; Yazyev, O.; Austin, A. J.; Cammi, R.; Pomelli, C.; Ochterski, J. W.; Martin, R. L.; Morokuma, K.; Zakrzewski, V. G.; Voth, G. A.; Salvador, P.; Dannenberg, J. J.; Dapprich, S.; Daniels, A. D.; Farkas, O.; Foresman, J. B.; Ortiz, J. V.; Cioslowski, J.; Fox, D. J. (2009) Gaussian 09, Revision D01. Gaussian Inc., Wallingford, CT.
- <sup>18</sup> (a) Becke, A. D. A New Mixing of Hartree-Fock and Local Density-functional Theories. *J. Chem. Phys.* **1993**, *98*, 1372-1377. (b) Becke, A. D. Density-Functional Thermochemistry. III. The Role of Exact Exchange. *J. Chem. Phys.* **1993**, *98*, 5648-5652. (c) Lee, C.; Yang, W.; Parr, R. G. Development of the Colle-Salvetti Correlation-energy Formula into a /functional of the Electron Density. *Phys. Rev. B* **1988**, *37*, 785-789. (d) Greer, E. M.; Kwon, K. Overview of Computational Methods for Organic Chemists. *In: Applied Theoretical Organic Chemistry*; Tantillo, D. J.; Ed.; World Scientific, 2018, 37-39.
- <sup>19</sup> Dennington, R.; Keith, T.; Millam, J. (2009) GaussView 5. Semichem Inc, Shawnee Mission KS.
- <sup>20</sup> Fukui, K. The Path of Chemical Reactions—The IRC Approach. *Acc. Chem. Res.* **1981**, *14*, 363-368.